Intercomparison of Landsat OLI and Terra ASTER solar reflective calibrations using the Radiometric Calibration Network data from Railroad Valley, Nevada

M. Yarahmadi, K. Thome, B. Wenny, J. Czapla-Myers, M. Tahersima, et al.

M. Yarahmadi, K. J. Thome, B. N. Wenny, J. Czapla-Myers, M. Tahersima, N. Voskanian, S. Eftekharzadeh, "Intercomparison of Landsat OLI and Terra ASTER solar reflective calibrations using the Radiometric Calibration Network data from Railroad Valley, Nevada," Proc. SPIE 12685, Earth Observing Systems XXVIII, 1268515 (4 October 2023); doi: 10.1117/12.2677409

SPIE.

Event: SPIE Optical Engineering + Applications, 2023, San Diego, California, United States

Intercomparison of Landsat OLI and Terra ASTER solar reflective calibrations using the Radiometric Calibration Network data from Railroad Valley, Nevada

M. Yarahmadi *[a], K.J. Thome [b], B.N. Wenny [a], J. Czapla-Myers [c], M. Tahersima [a], N. Voskanian [a], S. Eftekharzadeh [a]

[a] Science Systems & Applications, Inc., 10210 Greenbelt Road, Lanham, MD 20706, USA; [b] NASA Goddard Space Flight Center, 8800 Greenbelt Road, Greenbelt, MD 20771, USA; [c] College of Optical Sciences, University of Arizona, Tucson, AZ 85721, USA

ABSTRACT

This paper presents an intercomparison study between the Advanced Spaceborne Thermal Emission and Reflection Radiometer (ASTER) and Landsat 8 Operational Land Imager (OLI) using data from the Radiometric Calibration Network (RadCalNet). The study evaluates the radiometric performance and agreement between ASTER and Landsat 8 OLI, focusing on their spectral bands relevant for vegetation analysis and land cover classification. The analysis includes the assessment of data quality, uncertainties, and factors influencing the measurements. The results demonstrate the usability of RadCalNet in evaluating the accuracy and reliability of remote sensing data. The findings contribute to our understanding of the strengths and limitations of ASTER and Landsat 8 OLI, supporting informed decision-making in environmental monitoring and resource management. Overall, the intercomparison study provides valuable insights into the capabilities and limitations of ASTER and Landsat 8 OLI, highlighting the importance of RadCalNet in assessing the radiometric performance of remote sensing sensors. The results from the Railroad Valley RadCalNet show that the site is suitable for sensors with spatial resolutions as small as 15 m. The comparison between ASTER and OLI demonstrates that the recent update to the ASTER radiometric calibration provides results that are in agreement with Landsat 8 OLI to well within the absolute radiometric uncertainties of both sensors.

Keywords: remote sensing, intercomparison, ASTER, Landsat 8 OLI, Radiometric Calibration Network, RadCalNet

1. INTRODUCTION

Remote sensing is a technology that enables us to gather information about the Earth's surface and atmosphere without physical contact. It has revolutionized our ability to study and monitor the Earth's surface, providing scientists, researchers, and decision-makers with unprecedented amounts of data and insights about our planet [1]. Two remote sensing platforms for these purposes include the Landsat 8 satellite, which captures multispectral images of the Earth, and the Terra satellite, which carries various scientific instruments, including the high-resolution imaging instrument known as ASTER.

The Advanced Spaceborne Thermal Emission and Reflection Radiometer (ASTER) is a joint project between NASA and the Japanese Ministry of Economy, Trade, and Industry (METI), launched in 1999 as part of the Terra platform [2]. The instrument is on a sun-synchronous orbit, with an equator crossing time of approximately 10:30 AM. It's important to note that ASTER is not continuously imaging and must be tasked to collect data. ASTER is a multispectral sensor with a 60-km swath that operates in the visible to thermal infrared regions of the electromagnetic spectrum using three distinct sensors. ASTER has three bands as part of its visible and near infrared (VNIR) camera with wavelengths of 0.52 μm – 0.60 μm (green), 0.63 μm – 0.69 μm (red), and 0.76 μm – 0.86 μm (near infrared) and a spatial resolution of 15 m. ASTER VNIR data are available in two versions: Version 3 (V003) and Version 3.1 (V031) which was released in 2016 to make adjustments to the radiometric calibration coefficients. Version 3.1 also includes improvements to the atmospheric correction algorithms and updates to the digital elevation model (DEM) product [3].

The Landsat 8 satellite, launched in 2013, is part of the long-running Landsat program operated by NASA and the United States Geological Survey (USGS) [4]. Landsat 8 is also in a sun-synchronous orbit and has a swath width of 185 km collecting up to 700 scenes per day. The orbit of Landsat 8 is essentially the same as the Terra platform except that it is eight days out of phase and has an equator crossing time that is approximately 10:00 AM. Landsat 8 carries the Operational Land Imager (OLI) and the Thermal Infrared Sensor (TIRS), which provide multispectral data. The OLI

*mehran.yarahmadi@nasa.gov

Earth Observing Systems XXVIII, edited by Xiaoxiong (Jack) Xiong, Xingfa Gu, Jeffrey S. Czapla-Myers, Proc. of SPIE Vol. 12685, 1268515
© 2023 SPIE · 0277-786X · doi: 10.1117/12.2677409

sensor has four VNIR bands with wavelengths of 0.43 μm – 0.45 μm (coastal aerosol), 0.45 μm – 0.51 μm (blue), 0.53 μm – 0.59 μm (green), and 0.64 μm – 0.67 μm (red), as well as a fifth VNIR band with a wavelength of 0.85 μm – 0.88 μm (near infrared) with 30-m spatial resolution.

Both ASTER and OLI, along with other Landsat sensors, have been key providers of data used for vegetation analysis and land cover classification that is important for monitoring changes in plant growth, biomass, and water content, as well as for a wide range of environmental and societal applications. The green and red bands are particularly useful for distinguishing between different types of vegetation and for estimating vegetation cover and productivity, while the near infrared band is sensitive to changes in vegetation water content and can be used to monitor drought conditions, soil moisture, and plant stress. Additionally, the near infrared band is commonly used in vegetation indices such as NDVI, which can provide a measure of vegetation health and productivity [5]. The availability of data from multiple sensors with different spectral bands and resolutions is critical for advancing our understanding of the Earth's surface and changes over time, and for supporting a wide range of environmental and societal applications. Comparing the performance of these bands across the two sensors, ASTER and Landsat 8 OLI, provides the opportunity to improve the agreement across the sensors providing users with a more comprehensive view of the Earth's surface and changes over time, which is essential for many environmental and societal applications, such as agriculture, forestry, land-use planning, and natural resource management.

Figure 1 shows the relative spectral response (RSR) of the Landsat 8 OLI and ASTER sensors in the 400 nm to 1000 nm range. Both sensors have similar spectral responses in the shared spectral regions, although there are some differences in center wavelength and band width. For example, the green band of ASTER is slightly wider than that of OLI with a slightly shorter center wavelength. Another example is the near infrared band of ASTER which is broader than that of OLI but at a shorter center wavelength. Such a band shape can be beneficial for monitoring vegetation water content, but the OLI band was able to take advantage of improved sensor technology to allow for a narrower band that was placed to reduce effects caused by an absorption feature from atmospheric water vapor. The challenge for the users is to ensure that changes in the radiometric response of the sensors do not impact efforts to combine data from the two sensors.

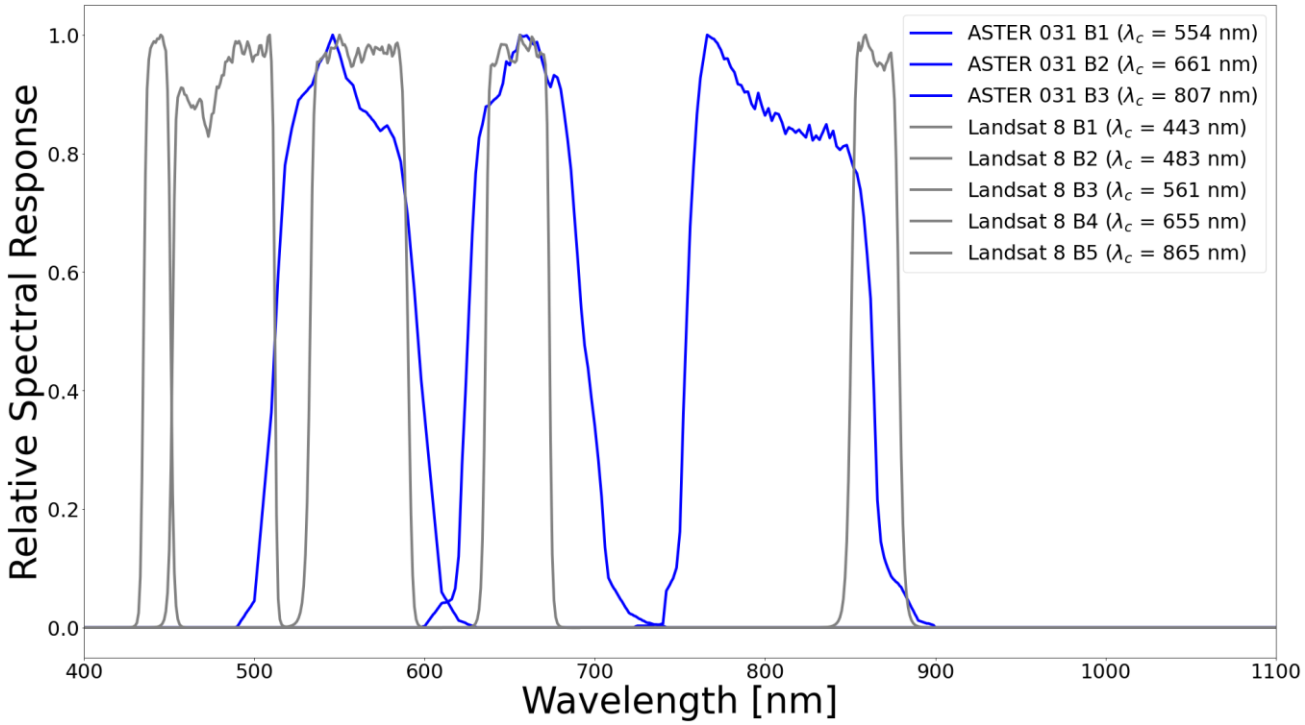

Figure 1. Relative Spectral Response (RSR) curves for Landsat 8 OLI (in grey), and ASTER V031 (in blue). The band center wavelengths are indicated in the legend. RSR remained unchanged after the ASTER version upgrade.

Radiometric calibration is a key step in ensuring the accuracy of remote sensing data, as it corrects for variations in sensor response due to changes in the sensor's environment or aging of the sensor's components. RadCalNet, the Radiometric Calibration Network, is a network of sites established by the Infrared Visible Optical Sensors (IVOS) Subgroup of the Committee on Earth Observation Satellites (CEOS) Working Group on Calibration and Validation (WGCV). Its purpose is to provide traceable and consistent calibration of Earth observation sensors. The network includes multiple sites for the purpose of optical imager radiometric calibration in the visible to shortwave infrared (SWIR) spectral range [6]. One of the RadCalNet sites used for comparison is located at Railroad Valley, Nevada, USA, with the four-letter name RVUS. The site is centered at 38.497° N, 115.69° W, and the region of interest (ROI) is approximately 1 km² (1000 m × 1000 m). To ensure minimal uncertainties in the calibration process caused by path radiance, misregistration, spectral differences, temporal variability, view angle differences, aerosols, adjacency effects, and weather conditions, a suitable cross-calibration site must possess specific characteristics, such as high surface reflectance, spatial uniformity, flat spectral reflectance, temporal invariance of surface properties, near-Lambertian surface, high altitude, large size, arid region, and accessibility [7]. Railroad Valley Playa satisfies many of these criteria, and its relative homogeneity of surface reflectance over a large area is one of the primary reasons for its wide use as an absolute radiometric and cross-calibration site. The site is also located in a remote, unpopulated area, which minimizes the effects of urbanization and other land-use changes on the measurements. Figure 2 shows the overview of Railroad Valley as well as the 1 km^2 ROI used by RadCalNet.

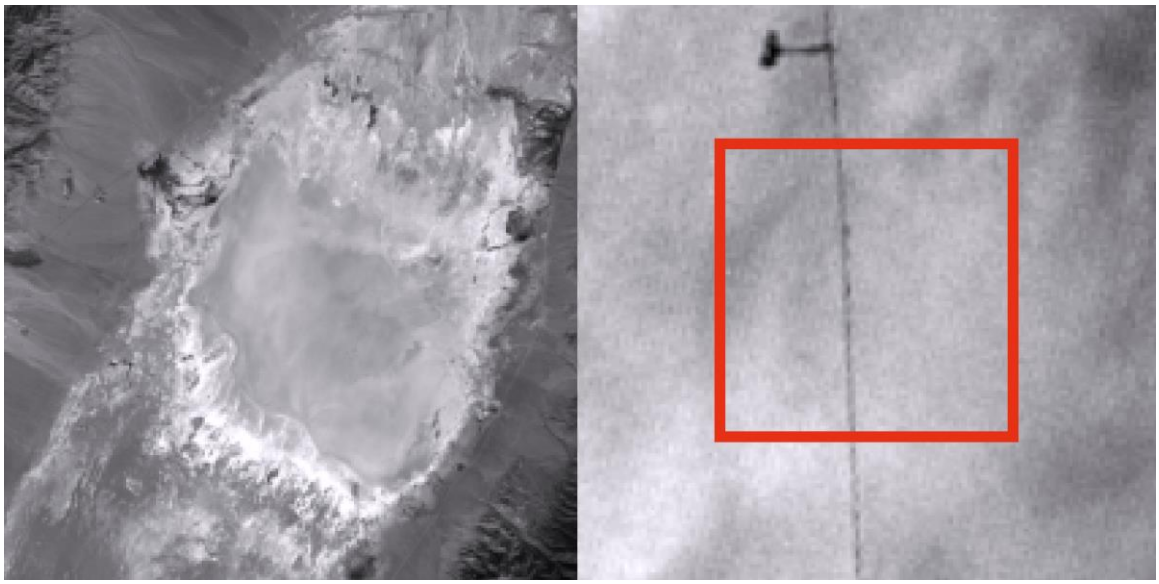

Figure 2. ASTER image of Railroad Valley (left) and 1 km2 ROI (right), using the ASTER green band. The red box outlines the 1000 m × 1000 m RadCalNet ROI.

One other advantage of RadCalNet is that SI-traceability of its data products allows different satellite sensors to be compared to each other even when they do not have identical spectral bands. Intercomparisons using RadCalNet sites also do not require coincident (or even near-coincident) imaging. The SI-traceability with a well-understood and peer-reviewed error budget allows RadCalNet sites to be used as a common reference. RadCalNet data from the Railroad Valley site offers a unique opportunity to compare the radiometric performance of ASTER and Landsat 8 OLI as well as to evaluate the test site itself. The current work provides an intercomparison between ASTER and Landsat 8 OLI using RadCalNet data. The differences and similarities in the behavior of the calibration of the two sensors are assessed. The results from this study show that the Railroad Valley RadCalNet is suitable for sensors with spatial resolutions as small as 15 m while demonstrating that the recent update to the ASTER radiometric calibration provides results that agree with Landsat 8 OLI to well within the absolute radiometric uncertainties of both sensors.

2. METHODOLOGY

RadCalNet utilizes ground-based measurements and atmospheric data to predict top of atmosphere (TOA) reflectance or which can be used for calibrating satellite sensors [6]. This is accomplished by applying the MODTRAN radiative transfer code to calculate TOA reflectance values with associated uncertainties determined from a LUT-based approach [7].

At RadCalNet sites, operators provide nadir-viewing BOA reflectance data at 10 nm intervals between 400 nm and 2300 nm at 30 minute intervals from 09:00 to 15:00 local standard time. Atmospheric parameters such as surface pressure and temperature, water vapor, ozone, aerosol optical depth, and Angstrom coefficient are also provided.

The calibration of a selected sensor is determined by comparing the image data from the sensor collected over the RadCalNet site to the TOA reflectance from the RadCalNet processing close in time to the sensor imagery. The sensor pixels corresponding to the RadCalNet site are averaged and processed using conversion factors provided by the sensor team to determine the TOA reflectance value for a given spectral band. The spatial resolution of Landsat 8 OLI and ASTER differ, with Landsat 8 OLI having a pixel size of 30 m for the visible and near-infrared bands, and ASTER has a pixel size of 15 m for the same spectral range. Therefore, to cover the Railroad Valley site, an ROI of 33 × 33 pixels is used for OLI and 67 × 67 pixels for ASTER. The ROIs are centered at the specified RadCalNet site coordinates for Railroad Valley to ensure complete coverage of the site by remote sensing data.

This process generates a single TOA value for each spectral band, which is compared to the corresponding RadCalNet TOA reflectance value. Band-averaging of the RadCalNet TOA reflectance values across the RSR values shown in Figure 1 for both sensors ensures that differences in spectral response between Landsat 8 OLI and ASTER are taken into account.

2.1 Conversion of Digital Numbers to TOA Reflectance

Each pixel in a Landsat 8 OLI or ASTER image is represented by a digital number (DN) that must be converted to TOA reflectance based on formulations provided by the Landsat and ASTER teams. There is a two-step process for converting ASTER data to TOA reflectance where step 1 converts the DN values to TOA radiance using:

$$\text{TOA Radiance} = (\text{DN} \times \text{Multiplicative Scaling Factor}) + \text{Additive Scaling Factor} \quad (1)$$

The multiplicative scaling factor is a unitless number that converts raw DN values to radiance units, and the additive scaling factor is a bias correction factor. Radiance values are converted to TOA reflectance values using:

$$\text{TOA Reflectance} = (\pi \times \text{Radiance} \times d^2) / (\text{ESUN} \times \cos\theta_s) \quad (2)$$

where ESUN is the mean solar exoatmospheric irradiance for a given ASTER band and θ_s is the solar zenith angle provided in the metadata. The values of ESUN(λ) are taken from the WRC-based results from Thome et al [8].

The process for Landsat data is more straightforward since the provided DN is directly related to reflectance and the TOA reflectance is found using a single step:

$$\text{TOA Reflectance} = ((M_\varrho \times \text{DN}) + L_\varrho)/ \cos\theta_s \quad (3)$$

where M_ϱ is the reflectance multiplicative scaling factor for the spectral band, L_ϱ is the reflectance additive scaling factor for the spectral band.

2.2 Clear-Sky Sensor Scene Selection in Railroad Valley

Table 1 provides a detailed comparison of available matchups between clear-sky sensor images and RadCalNet data for January 2013 to December 2022. Clear-sky conditions were determined based on the cloud percentage scores provided in the sensor metadata. The table contains data for two processing versions of ASTER (ASTER V003 and ASTER V031) and Landsat 8 OLI. Landsat 8 OLI data is obtained from Collection 2 Level 1 products.

The "Available" column shows the total number of available clear-sky matchups for each sensor. To clarify, "matchup" refers to the comparison of radiometric measurements obtained by OLI/ASTER with those from RadCalNet when both sources have data available for Railroad Valley on the same day. Notably, Landsat 8 has the higher number of available

matchups at 75, while ASTER has 44. The lower number of available matchups for ASTER compared to Landsat 8 is partly due to the fact that ASTER must be tasked to collect data for specific areas or targets, while Landsat 8 is continuously acquiring data over the US. This means that Landsat 8 has more opportunities to capture data over a wider range of targets and therefore has more matchups available for intercomparison with other sensors.

To ensure accuracy, the collection time of the day for RadCalNet should be selected within 30 minutes of the sensor capture time. This means that the ground measurement time and the scene capture time should have a maximum time difference of 30 minutes. This is an important factor to consider as large time differences can introduce different atmospheric conditions and effects from changes in surface reflectance leading to higher uncertainties in the radiometric calibrations Recall that RadCalNet data are provided at 30-minute intervals, thus the ideal situation is that an ASTER or OLI collect should have less than a 15-minute difference in time for cases where the RadCalNet instrumentation is behaving well and atmospheric conditions are suitable for a calibration.

Table 1. Matchup statistics between clear-sky sensor images and RadCalNet data for ASTER and Landsat 8 OLI over Railroad Valley for January 2013 to December 2022.

sensor	launch	available	site mismatch	anomalous condition	good
ASTER 003	1999	44	9 (~ 20 %)	6 (~ 13 %)	29 (~ 66 %)
ASTER 031	1999	44	9 (~ 20 %)	6 (~ 13 %)	29 (~ 66 %)
Landsat 8 OLI	2013	75	0 (~ 0 %)	15 (~ 20 %)	60 (~ 80 %)

The subsequent two columns filter the matchups based on various factors that can affect the accuracy of radiometric intercomparison. The "site mismatch" column indicates the number of cases where the sensor imagery could not be readily matched with the RadCalNet test site. For ASTER, there are nine such cases (~20% of available matchups), while Landsat 8 did not have this issue. All nine ASTER instances corresponded to cases where the ASTER VNIR camera was pointed at a large off-nadir angle.

The "anomalous condition" column shows the number of matchups where the atmospheric conditions in Railroad Valley were flagged as anomalous by the site owners or there was an anomaly in surface conditions. These anomalies could be related to atmospheric parameters such as pressure, temperature, water vapor, ozone, aerosol optical depth, and the aerosol Angstrom coefficient or are flagged by the Railroad Valley site operator based on their assessment of the surface conditions during the matchup. For ASTER and Landsat 8 OLI, 13% and 20% of available matchups were affected by anomalous atmosphere, respectively.

Finally, the "Good" column shows the number of good scenes after applying filters, which have absolute uncertainties suitable for radiometric intercomparison between ASTER and Landsat. For ASTER and Landsat 8 OLI, 29 (66% of available matchups) and 60 (80% of available matchups) matchups were considered "good", respectively.

3. RESULTS AND DISCUSSIONS

Figure 3 shows the ratio of TOA reflectance of the sensor to the RadCalNet TOA reflectance for the two versions of ASTER and Landsat 8 OLI, presented in three separate graphs. The top graph displays the results for the green band of both ASTER and Landsat, while the middle and bottom graphs show the results for the red and near-infrared bands, respectively. A ratio of unity corresponds to the case where the reported TOA reflectance from the imagery agrees with the predicted values from RadCalNet.

The difference between the two ASTER versions is particularly noticeable for the red band, where version 3.1 produces higher at-sensor reflectance values, resulting in higher ratios compared to version 3. The use of ASTER V031 results in ratios that are more similar to those obtained from Landsat 8 OLI.

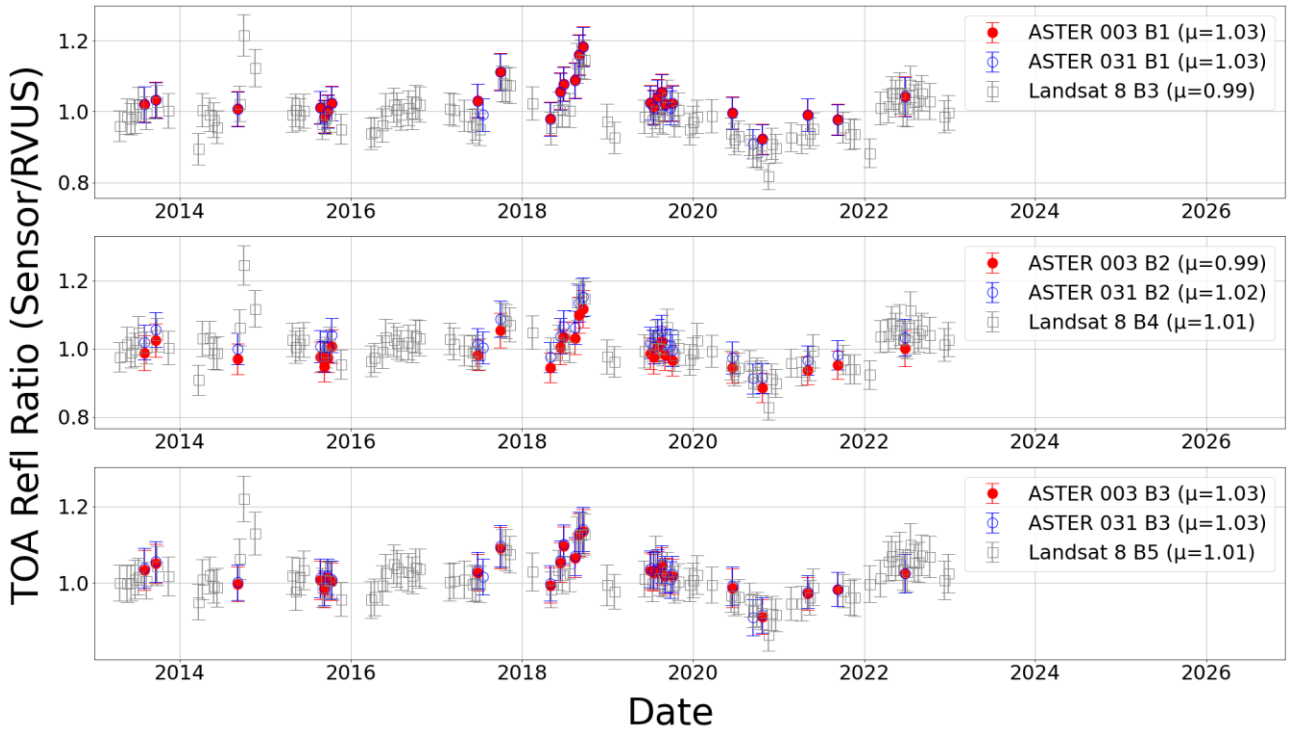

Figure 3. TOA reflectance ratios for ASTER V003, ASTER V031, and Landsat 8 OLI compared to RadCalNet over a 10 year period (January 2013-December 2022) for selected spectral bands. The ratios are shown for (top) green band, (middle) red band, and (bottom) near-infrared band of both ASTER and Landsat 8 OLI. The temporal mean ratio values for each band combination over the entire period are provided in the figure legend.

The graph shows that neither sensor indicates a significant change in radiometric response during the 10-year period shown and this agrees with the results from other work. One thing that can be seen in the figure is that changes in the ratio versus time show consistent behavior across both sensors during several periods indicating a possible RadCalNet-related effect on the retrieved ratios. For example, both ASTER and Landsat TOA reflectances show ratios >1 in August and September of 2018 and <1 in September and October of 2020. The effect is also consistent across all three spectral band regions suggesting that environmental factors at the Railroad Valley test site such as wildfires or land cover alterations may be affecting the model predictions for the RadCalNet TOA reflectance during these time periods. Further investigation is underway to assess possible causes. Additionally, it should be noted that for both sensors there are instances when TOA reflectance values from the sensors differ from the ground measurements by more than 4% which is a typical absolute uncertainty reported by RadCalNet for the Railroad Valley site.

To better understand the consistency of the TOA reflectance ratios across the spectral bands and for the two sensors, the temporal average and standard deviation values are calculated for the ratios. The temporal average and standard deviation provide a quantitative way to compare the results from the two sensors to evaluate their radiometric consistency and stability. Figure 4 presents the results for the two versions of ASTER and Landsat 8 OLI over Railroad Valley for images captured from January 2013 to December 2022. The data used for the averages and standard deviations is based on the ratios provided in Figure 3. Knowledge of the absolute radiometric uncertainties for both the RadCalNet and the ASTER and OLI sensor data allows for a combined uncertainty to be determined for the sensor to RadCalNet ratio. The absolute radiometric uncertainty (k = 1) for the ASTER and OLI are ~3% for the VNIR bands. The absolute radiometric uncertainty of the RadCalNet TOA reflectance results is reported at each wavelength for each RadCalNet data point. Assuming that the RadCalNet and sensor uncertainties are uncorrelated allows the combined uncertainty, u(y) to be calculated as [9].

$$u(y) = \sqrt{(u_s/s)^2 + (u_r/r)^2} \times y \quad (4)$$

where u_s is the absolute standard uncertainty of the sensors, u_r is the absolute standard uncertainty of the TOA reflectance results of RadCalNet, and y is TOA reflectance ratio.

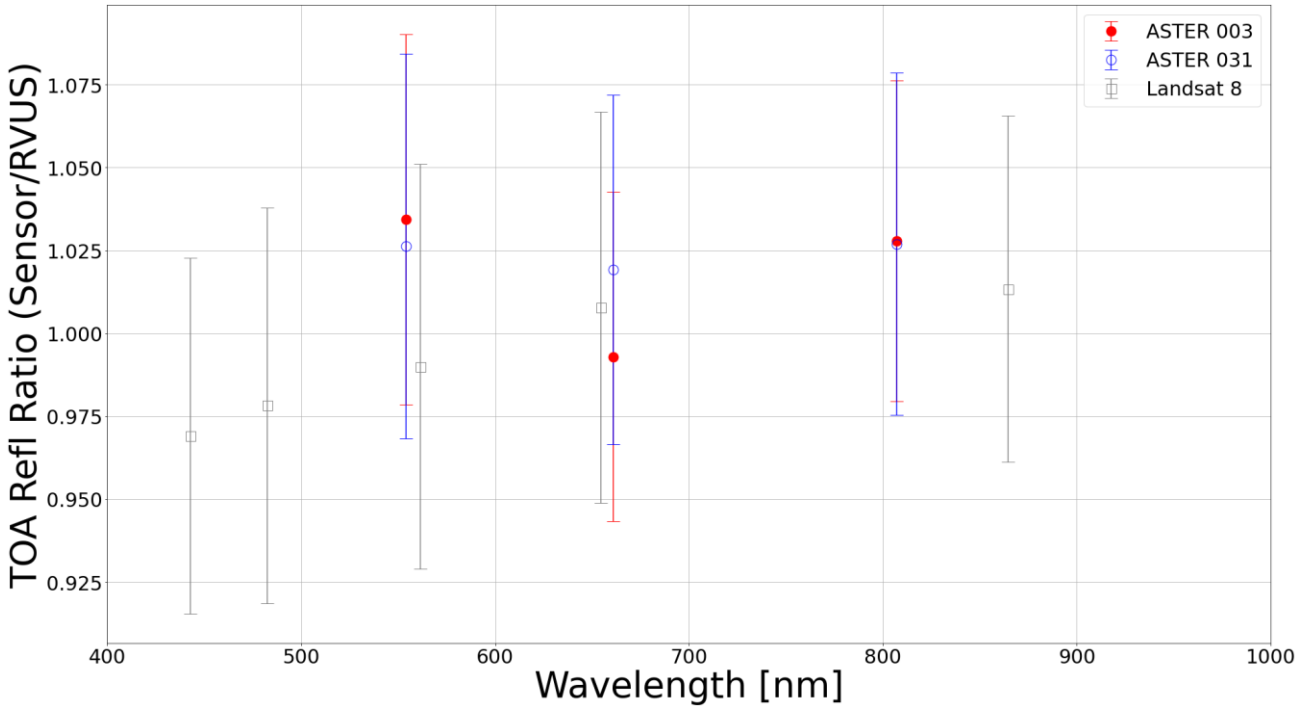

Figure 4. Temporal average of TOA reflectance ratios for two versions of ASTER and Landsat 8 OLI over RVUS from Jan 2013 to Dec 2022, with symbols representing average ratios and error bars showing standard deviations. The table displays values for band center wavelengths, temporal average ratios, and uncertainties for bands 1 to 3 of ASTER and bands 1 to 5 of Landsat 8 OLI.

Figure 4 shows that the reflectance ratios for green and near-infrared bands are similar between ASTER V003 and ASTER V031, while the ratio for the red band is higher for ASTER V031. This suggests that the upgrade from version 3 to 3.1 had a larger impact on the red band than the green or near infrared bands in this portion of the ASTER data record, resulting in higher predicted TOA reflectance in this band for the newer version.

The results shown in Figure 4 indicate that the reflectance ratios are comparable within their expected standard deviation. Moreover, the average ratio in all cases for the two sensors are within 4% of unity and this is well within the combined RadCalNet and sensor absolute radiometric uncertainties. A key result is that the ASTER (both V003 and V031) and OLI absolute radiometric calibrations agree with each other in comparable bands to within the combined uncertainties. The agreement is also true for comparisons with bands across the full spectral region. That is, one can conclude that all the Landsat spectral bands are consistent with all the ASTER spectral bands. Such a result is critical for applications that would use a combination of ASTER and Landsat spectral data.

The ASTER and Landsat 8 OLI satellite sensors have similar spectral bands that can be compared for identifying various features on the Earth's surface. ASTER Band 1 and Landsat Band 3 (green) have similar spectral response and can be used to differentiate vegetation from non-vegetation areas. ASTER Band 2 and Landsat 8 OLI Band 4 (red) have similar spectral response and can be used for soil mapping. Although ASTER Band 3 and Landsat 8 OLI Band 5 (near-infrared) have different spectral bandwidths and center wavelengths, they can still be used to identify different types of rocks and minerals. Overall, the band-to-band comparison of ASTER and Landsat 8 OLI provides valuable insights into various aspects of the Earth's surface and helps in diverse applications such as geology, forestry, agriculture, and environmental monitoring.

A technique called "double ratios" can be used to mitigate possible biases in the intercomparison results between sensors shown in Figure 4. The method in this case involves dividing the average ratios shown in Figure 4 to reduce systematic

effects from absolute radiometric uncertainty from the RadCalNet data sets. In Figure 5, the double ratios of the calibration coefficients are shown for both versions of ASTER and Landsat 8 OLI, with RVUS as the reference. The results are shown for the average wavelengths of the ASTER and OLI bands used in the double ratio. The combined standard uncertainty for the double ratio is computed in similar fashion as equation (4) and shown as the error bars in Figure 5 ranging from 7.0% to 8.7%. A double ratio of one implies agreement between the two sensors being compared. The figure shows that the double ratio intercomparison results agree within the combined standard uncertainties of this intercomparison.

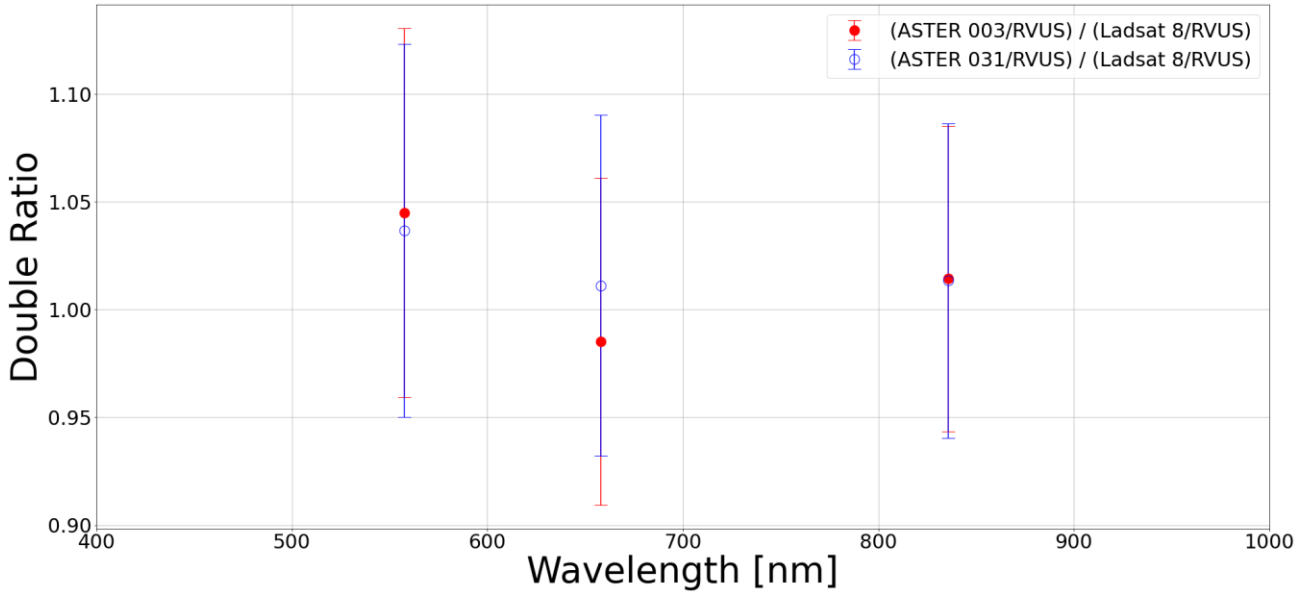

Figure 5. Double ratios for ASTER/Landsat 8 OLI for two versions of ASTER over RVUS from Jan 2013 to Dec 2022, with symbols representing average ratios and error bars showing the uncertainty.

4. CONCLUSION

In conclusion, RadCalNet is shown to be a valuable tool for intercomparison between ASTER and Landsat 8 OLI. One important result is that this work confirms that the Railroad Valley RadCalNet site is suitable for use with sensors having spatial resolution as small as 15 m. The SI-traceable uncertainties of RadCalNet allow the TOA reflectances computed by ASTER and OLI to be compared to a standardized and traceable calibration reference. The intercomparison results show that both ASTER and OLI agree with RadCalNet to well within the combined absolute uncertainties of the sensor and the test site data. The results also show that both the V003 and the updated V031 ASTER data agree with the RadCalNet results. The temporal results from the RadCalNet comparisons show that neither ASTER nor OLI data products are changing time in a systematic fashion indicating that the radiometric calibration of both sensor's radiometric calibrations are well understood by their respective instrument teams. Comparisons of the 10-year averages of the ratio to RadCalNet indicate that OLI and ASTER data agree to within 7% in all spectral bands and 4% in the closely matched green, red, and near infrared bands. In summary, RadCalNet continues to play a crucial role in the intercomparison, calibration, and validation of remote sensing sensors and users can be confident that applications relying on the ASTER and OLI sensors will not be affected by absolute radiometric calibration differences in the sensors.

REFERENCES

[1] T. Lillesand, R. W. Kiefer and J. Chipman, Remote Sensing and Image Interpretation, John Wiley & Sons, 2015.
[2] H. Yamamoto, J. Czapla-Myers and S. Tsuchida, "Validation of Aster VNIR Radiometric Performance Using the Reflectance-Based Vicarious Calibration Experiments and RadCaTS Data," IGARSS 2022-2022 IEEE International Geoscience and Remote Sensing Symposium, pp. 4316-4319, 2022.

[3] D. Roy, M. Wulder, T. Loveland, C. Woodcock, R. Allen, M. Anderson, D. Helder, J. Irons, D. Johnson, R. Kennedy and T. Scambos, "Landsat-8: Science and product vision for terrestrial global change research," Remote sensing of Environment, vol. 145, pp. 154-172, 2014.
[4] G. Gutman, S. Skakun and A. Gitelson, "Revisiting the use of red and near-infrared reflectances in vegetation studies and numerical climate models," Science of Remote Sensing , vol. 4, 2021.
[5] M. Bouvet, K. Thome, B. Berthelot, A. Bialek, J. Czapla-Myers, N. P. Fox, P. Goryl, P. Henry, L. Ma, S. Marcq, A. Meygret, B. N. Wenny and E. R. Woolliams, "RadCalNet: A radiometric calibration network for Earth observing imagers operating in the visible to shortwave infrared spectral range," Remote Sensing, vol. 11, 2019.
[6] K. P. Scott, K. J. Thome and M. R. Brownlee, "Evaluation of Railroad Valley Playa for use in vicarious calibration," in SPIE Proceedings, 1996.
[7] B. N. Wenny, and K. J. Thome, "Look-up table approach for uncertainty determination for operational vicarious calibration of Earth imaging sensors." Applied Optics, vol. 6, pp. 357-1368, 2022.
[8] K. J. Thome, S. F. Biggar and P. N. Slater, "Effects of assumed solar spectral irradiance on intercomparisons of Earth-observing sensors," in Proceedings SPIE, 2001.
[9] J. C. G. M. Jcgm, "Evaluation of measurement data—Guide to the expression of uncertainty in measuremen," Int. Organ. Stand. Geneva ISBN, 2008.